

Determination of the Kinetic Parameters of the Diffusion-Controlled Reaction of the Fluorescence Quenching of Photoexcited Anthracene with Carbon-Tetrabromide

01 May 2017

Department of Chemistry, Hunter College of the City University of New York

Running Title: *Kinetics of a Diffusion-Controlled Reaction*

INTRODUCTION

For a system containing two reactants that are electrically neutral, the reactants can move in independent random motion throughout the medium. When a system achieves a probabilistic state in which the two reactants encounter each other (an encounter complex), with a separation distance equaling the sum of their molecular radii, the encounter complex will be either caged by solvent molecules or its individual components will be diffused and separated back into the solvent. If the latter does not occur, the encounter complex can be eliminated via reaction between the constituent component reactant molecules. The elimination of the encounter complex by reaction can be approximated with a steady-state concentration model, which allows the rate of reaction to be written as

$$\text{Rate} \simeq k_1 k_2 [A - B] = \frac{k_1 k_2}{k_{-1} + k_2} [A][B] \quad (1)$$

where we have $[A - B]$ as the concentration of the encounter complex between reactants A and B , k_1 as the rate constant for the formation of the encounter complex, k_{-1} as the rate constant for the separation/dissociation of the encounter complex, and k_2 as the rate of reaction between A and B in complex to form the reaction products. When the rate of the reaction is significantly greater than the rate of separation $k_2 \gg k_{-1}$, we observe a second-order rate constant k_{obs} that is dependent on the movement of A and B towards each other, and a relatively instant reaction

occurring with A and B reaching the collision radius.

$$k_{\text{obs}} = \frac{k_1 k_2}{k_{-1} + k_2} \quad (2)$$

This type of reaction that occurs rapidly and with a negligible activation energy barrier is considered to be a diffusion-controlled (or diffusion-limited) reaction. In contrast to a chemically controlled reaction, in which the rate of reaction is based on a potential barrier that must be surmounted – the “activation energy” – between a reaction’s reactants and its products, the rate of diffusion-controlled reactions is determined by the dynamics of the reactants transport through a medium. Thus, for a diffusion-controlled reaction to proceed at a reasonable rate, the rate of mass transport through the medium must be appreciable; and diffusion of the reacting molecules determines the rate, for when the molecules reach their collision radius, they nearly instantly react. Fick’s law (eq. 3) describes the flux of, or diffusion of dn number of molecules through a unit area A , per unit time, dt , in the direction z , as a product of the concentration gradient of the system and a proportionality constant D , the diffusion coefficient.

$$\frac{1}{A} \frac{dn}{dt} = -D \frac{dC}{dz} \quad (3)$$

The ability for a molecule to diffuse in the medium described in Fick’s law shows the dependence on the concentration gradient, which acts as the driving force for the mass transport. This flux of the reactant that Fick’s law describes

directly affects the rate of the diffusion-controlled reaction. However, this rate initially has a time dependent factor as well. For a diffusion-controlled reaction, the rate constant becomes a constant after a transient term (as seen as part of eq. 4), dependent on time, approaches a limit where it becomes negligible. However, for an initial state, the transient term accounts for the reactant molecules starting at distances near or at the collision radius, bypassing the need for diffusion through the solvent.

$$k_1 = \frac{4\pi RDN_A}{1000} \left[1 + \frac{R}{\sqrt{\pi D t}} \right] \quad (4)$$

where R is the collision radius of the reacting molecules, and the part in brackets as the transient term. Once all of these close molecules have reacted, the flux reaches a steady state and the limiting behavior applies, resulting in the reaction rate being dependent on a constant diffusion coefficient.

$$\lim_{t \rightarrow \infty} k_1 = \frac{4\pi RDN_A}{1000} \quad (5)$$

The collision radius and the diffusion coefficient are often found indirectly through the use of the Stokes-Einstein-Smoluchowski (SES, eq. 6) equation, which allows for the rate constant to be approximated using the solvent's viscosity, η , which is directly related to the mass transport, as described in *Viscosity of Binary Solutions*.

$$k = \frac{8R_G T}{3000\eta} \quad (6)$$

Here, R_G is the universal gas constant and T , the temperature. The SES equation can be applied when the two reacting molecules differ in size and are relatively larger than the solvent molecules.

An example of a diffusion-controlled reaction is the quenching of electronically excited anthracene, a natural fluorophore, by carbon-tetrabromide. The quenching reaction is intrinsically fast, essentially instantly at the collision radius, and with no necessary activation energy. The reaction itself is easily monitored via fluorescence spectroscopy, as it only takes place

when exposed to light, and the concentration of electrically excited molecules can be measured as related to their intensity of fluorescence. Electronically excited anthracene is quenched by carbon-tetrabromide through electronic charge transfer to the highly electronegative quencher in a bimolecular quenching reaction. However, in this experiment, a much greater concentration of quencher is used compared to the concentration of the excited anthracene, and the rate limiting diffusion controlled quenching step becomes pseudo first order. Thus, the ratio of fluorescence intensity of just anthracene, I_0 , to the intensity with the quencher added, I , gives an expression relating this ratio to the concentration of the quencher and the pseudo first order rate constant.

$$\frac{I_0}{I} = k_q \tau_0 [Q] + 1 \quad (7)$$

Where τ_0 , the fluorescence lifetime is derived from the reciprocal, $1/(k_r + k_{nr})$, from the radiative and non-radiative rate constants of the anthracene's fluorescence. Equation 7, the steady-state Stern-Volmer relation allows for the linearized plot of intensity ratio vs. concentration, providing a way for the pseudo first order rate constant to be extrapolated via linear regression analysis, taking advantage of the relationship to k_1 though the non-consideration of the transient effects.

As previously discussed, there is a time dependence of the rate constant due to the initial transient effects from nearby molecules that bypass the need to diffuse towards each other to react. This transient term is accounted for by combining equation 4 and equation 7, and rederiving a new Stern-Volmer equation (eq. 8), where the quenching reaction is not a function of time, but rather a function of concentration.

$$\frac{I_0}{I} = \frac{\left[1 + 4\pi RD \left(\frac{N_A}{1000} \right) \tau_0 [Q] \right]}{Y} \quad (8)$$

Where Y is defined as

$$Y = 1 - \frac{b\sqrt{\pi}}{\sqrt{a}} e^{\left(\frac{b^2}{a} \right)} \operatorname{erfc} \left(\frac{b}{\sqrt{a}} \right) \quad (8Y)$$

$$a = \frac{1}{\tau_0} + \frac{4\pi R D N_A}{1000} [Q] \quad (8a)$$

$$b = \frac{4R^2 \sqrt{\pi D} N_A}{1000} [Q] \quad (8b)$$

Unlike the linearized Stern-Volmer expression, the transient effects cause equation 8 to exhibit a non-linear curve, not based on any time dependence, but as a result of nearby molecules that instantly react (without having to diffuse towards each other) when subjected to excitation by the fluorescence spectrometer. The tangent line slopes of the non-linear curve show the fast rates for large quencher concentrations and slow rates for low quencher concentrations.

By observing the intensity of fluorescence at a fixed wavelength for varying concentration of carbon-tetrabromide, an experimental Stern-Volmer quenching curve can be plotted, and compared to a theoretical plot based on equation 8, thus allowing us to extrapolate a collision radius via non-linear regression analysis.

Similarly, the steady-state Stern-Volmer plot can be compared with the SES equation to determine the kinetic parameters, specifically the rate constant, of the diffusion-controlled fluorescence quenching reaction.

METHODOLOGY

From provided stock solutions of purified anthracene, diluted to a concentration of $\sim 1.00 \times 10^{-4}$ M in *n*-hexane, and $\sim 1.50 \times 10^{-2}$ M CBr₄, diluted in the former, a series of dilutions were prepared to make 5 mL samples of AN/CBr₄ samples, with dilutions increasing incrementally by 10% from 0% to 100%. Care was taken to prevent any exposure to light, as the fluorescence quenching reaction between anthracene and carbon-tetrabromide is “activated” by electron excitation, so each sample was wrapped in aluminum foil. Rather than combining the two stock solutions in the appropriate amounts immediately, fluorometric data was recorded for the pure anthracene amount, then with both

amounts combined, using a F-2710 FL spectrophotometer.

The pure anthracene component of the dilution was added to a quartz cuvette of 1cm path length, and deaerated with nitrogen gas for 2 minutes, as the presence of dissolved atmospheric oxygen would affect the reaction (being diffusion controlled). The fluorescence intensity was then measured using a fluorescence spectrometer, set to scan between 350 nm and 500 nm, just above the excitation wavelength of 280 nm, and with a scan speed of 3000 nm/min and a slit width of 2.5 nm. The height of the highest peak (the second) was recorded as the initial intensity I_0 for the corresponding concentration of CBr₄ that would then be added. Once the CBr₄ component was added, the mixture was deaerated for another 2 minutes before an identical scan was taken. This was repeated for each dilution sample, with the cuvette being washed with the stock anthracene solution between each sample scan. All intensities were recorded at the second peak, at 398 nm, the observed maximum fluorescence wavelength for anthracene.

RESULTS AND DISCUSSION

The analysis of experimental data was carried out in order to determine the radius of collision and the observed rate constant of the diffusion-controlled quenching reaction through several methods, and compared to theoretical values found through non-linear regression analysis.

As previously stated, fluorescence intensities (via peak heights) were measured at 398 nm, the highest fluorescence of the electronically excited anthracene. Measurements were taken before the carbon-tetrabromide quencher was added, denoted as I_0 , as well as after, denoted as I . This data was then tabulated, and the ratio of intensities I_0/I was plotted as a function of the carbon-tetrabromide concentration $[Q]$.

I_0	I	I_0/I	[Q] (M)
33.41	33.41	1.000	0.0000
27.23	23.54	1.157	0.0015
34.40	17.97	1.914	0.0030
39.66	13.38	2.964	0.0045
40.86	8.659	4.719	0.0060
35.71	8.802	4.057	0.0075
35.57	4.561	7.799	0.0090
36.23	3.085	11.74	0.0105
37.04	1.845	20.08	0.0120
35.57	1.024	34.74	0.0135
35.57	0.441	80.66	0.0150

TABLE 1. Fluorescence Intensity Measurements of Anthracene (I_0) and Anthracene/CBr₄ (I) with Corresponding CBr₄ Concentrations [Q].

It should be noted that the I_0 values measured for concentrations of 0.0090, 0.0135, and 0.0150 were taken as averages of the rest of the I_0 values to account for inconsistent values, discussed in detail at the end of this section regarding experimental error.

The plot of the ratio of intensities I_0/I as a function of the carbon-tetrabromide concentration [Q] produced our first Stern-Volmer Quenching Curve, the experimental curve, seen as the red curve in figure 1. This experimental Stern-Volmer quenching curve was then compared with the corresponding limits of the SES (eq. 6) equation and equation 8 to determine the agreement of the observed rate constant k_q and the collision radius R .

The following parameters were used in the SES equation to determine a rate constant k :

Reference Parameter	Value (units)
Universal Gas Constant R_G	$8.31 \times 10^7 \text{ ergs} \cdot \text{mol}^{-1} \cdot \text{K}^{-1}$
Viscosity of n-hexane at 25°C	0.003 Poise
Temperature	298 K

TABLE 2. Reference Parameters used in the SES Eq.

The SES equation yielded a theoretical rate constant for a diffusion-controlled reaction carried out in a medium of η viscosity at temperature T , $2.20 \times 10^{10} \text{ dm}^3 \cdot \text{mol}^{-1} \cdot \text{s}^{-1}$. This rate constant was then used with equation 5 (without

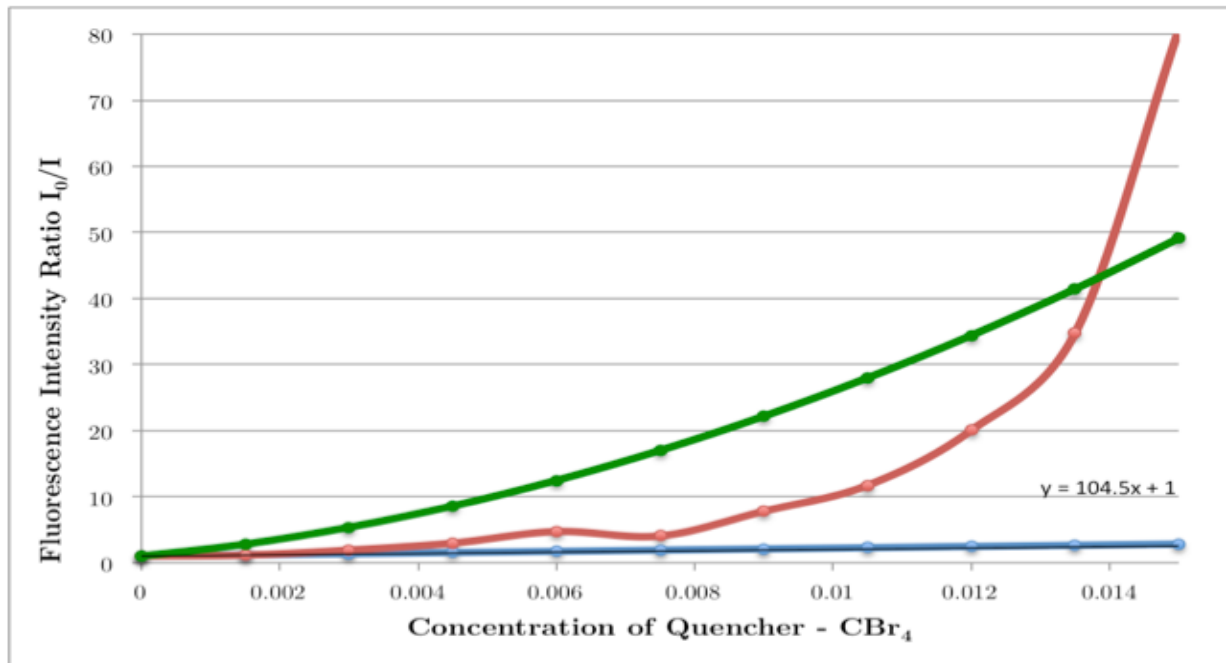


FIGURE 1. Stern-Volmer Quenching Curves. The red curve corresponds to the experimental data, the black line corresponds to the low experimental concentration tangent line, the blue curve corresponds to the steady-state, linearized quenching curve, and the green line corresponds to the theoretical curve.

consideration of the transient term) in order to calculate a value for the collision radius, 9.53 Å. In order to use equation 5, we calculated a diffusion coefficient D for hexane at 25°C as $3.06 \times 10^{-5} \text{ cm}^2 \cdot \text{s}^{-1}$, using a proportion relationship to η/T and the known diffusion coefficient of heptane at 25°C, $4.35 \times 10^{-5} \text{ cm}^2 \cdot \text{s}^{-1}$, obtained from the Ware and Novros study.

In addition, this rate constant, used along with equation 7, allowed us to plot a theoretical steady-state, pseudo-first order Stern-Volmer quenching plot. Given a constant Stern-Volmer constant, K_{SV} ($k\tau_0$), from a given life time of $5.52 \times 10^{-9} \text{ s}$, of $1.22 \times 10^2 \text{ dm}^3 \cdot \text{mol}^{-1}$, a linearized steady state plot was produced, depicted as the blue plot in figure 1. It is observed that this linearized Stern-Volmer curve (blue) corresponds very closely to the experimental curve (red) at very low concentrations (below $\sim 0.002 \text{ M}$) of CBr_4 . This corresponds with the theory behind equation 7, where the absence of transient effects occurs due to the static quenching of already nearby CBr_4 molecules that do not have to diffuse through the solvent, and once they are used, the rate of reaction remains low.

When the transient terms are ignored, we see this relationship again, in which the low concentration of the quenching CBr_4 corresponds to the falling out of the transient term. In order to do this, a trend line was added to the experimental plot (black line in figure 1) to approximate the tangent line of the experimental curve at low concentrations of CBr_4 , and thus, approximate the conditions in which the transient effects are not considered. The slope of this tangent line was found to be 104.5, which we used as a Stern-Volmer constant, to determine another value for the observed steady-state rate constant, $1.89 \times 10^{10} \text{ dm}^3 \cdot \text{mol}^{-1} \cdot \text{s}^{-1}$. Compared to the rate constant determination from the SES equation, a 14.1% difference was calculated. This value of k was then used with equation 5 to find another value for the collision radius, 8.19 Å, corresponding to a 14.1% difference as well to our

collision radius value determined using the SES equation's rate constant k .

The transient effects of the initial nearby quenching CBr_4 molecules were then taken into account by using equation 8. As previously described, this equation would generate a non-linearized Stern-Volmer quenching plot in which the transient effects are included, but in terms of the varying concentration of the quenching molecule than the time dependence of the rate constant. Theoretical values of I_0/I based on this equation, and the concentrations of CBr_4 that were experimentally measured, were calculated and plotted as the green curve on figure 1. Non-linear regression analysis was then employed utilizing the built in solver add-on in Microsoft excel to extrapolate a collision radius, which shows up in this equation seven times (shown below), to minimize the sum of square errors compared to our experimental values of I_0/I .

$$\frac{I_0}{I} = \frac{\left[1 + 4\pi RD \left(\frac{N_A}{1000} \right) \tau_0 [Q] \right]}{1 - \frac{\left(\frac{4R^2 \sqrt{\pi D} N_A [Q]}{1000} \right) \sqrt{\pi}}{\sqrt{\left(\frac{1}{\tau_0} + \frac{4\pi RD N_A [Q]}{1000} \right)}} e^{\left(\frac{\left(\frac{4R^2 \sqrt{\pi D} N_A [Q]}{1000} \right)^2}{\left(\frac{1}{\tau_0} + \frac{4\pi RD N_A [Q]}{1000} \right)} \right)} \frac{2}{\sqrt{\pi}} \int_0^{\left(\frac{4R^2 \sqrt{\pi D} N_A [Q]}{1000} \right)} e^{-t^2} dt}$$

Although several problems were encountered with the built in solver add-on during the regression analysis, a system of trial and error was employed to manually determine a collision radius of 38.3 Å, much greater than the previously determined values in which the transient effects were ignored. Below is a summary table of the values calculated in this experiment in the aforementioned various ways.

Parameter	Equation	Value
k	5	$2.2 \times 10^{10} \text{ dm}^3 \cdot \text{mol}^{-1} \cdot \text{s}^{-1}$
k	7	$1.89 \times 10^{10} \text{ dm}^3 \cdot \text{mol}^{-1} \cdot \text{s}^{-1}$
R	5	9.53 Å
R	Exp. and 5	8.19 Å
R	8	38.3 Å

TABLE 3. Compilation of Calculated Rate Constants and Collision Radii Determined Throughout this Experiment and Data Analysis.

While the rate constants agree to an appreciable amount (especially considering that they are both determined without consideration of

the transient effects), the collision radii exhibit a large difference. Although a large difference is observed between the third value of R and the first two, 75.1% and 78.6% respectively, either could be valid. The issues with the first two determinations were that the transient effects were not taken into consideration, and thus the equations that modeled this diffusion-controlled reaction, are not an entirely accurate approach to calculate the collision radius. However, that is not to say that the last value of R , determined with equation 8, was particularly more accurate. As observed in figure 1, the experimental curve and the theoretical curve do not align very well, and a corresponding sum of square errors value of 1.99×10^3 is disconcerting to say the least. Based on the experimental sources of error, including variation in pressure and time of the deaerating steps between each measurement, and initial exposure to light sources that were unavoidable, the large difference in the experimental curve and the optimized theoretical curve could be explained. Although great care was taken to avoid exposure to external light sources that would excite the anthracene molecule, triggering the quenching reaction, and a consistent deaeration, the large curvature of the experimental curve indicates that our theoretical determination holds more weight.

Based on available data of CBr_4 and anthracene's crystalline structures, the monoclinic cells provide molecular radii of approximately 5.5 \AA and 8.5 \AA respectively. And since the collision radius is the sum of the molecular radii of the colliding molecules, the actual collision radii between anthracene and CBr_4 should be $\sim 14 \text{ \AA}$, similar in magnitude (albeit very off in accuracy) to our determined values.

QUESTIONS & FURTHER THOUGHTS

The anthracene fluorescence quenching is diffusion-controlled rather than chemically controlled due to the intrinsic electron affinity of the highly coordinated and electronegative CBr_4

molecule, and the delocalization of the aromatic π electrons in excited anthracene. The electron transfer of the quenching reaction occurs with almost no potential barrier (activation energy) as it is a "physical" reaction (in the transfer of electrons), rather than a chemical change. Thus, the rate depends on the diffusion of these molecules to the close proximity – collision radius – of the reaction, in which the molecules are close enough so that the electron transfer might occur. Therefore, once the molecules are close enough (at their collision radius), either through diffusing towards each other in the medium, or initially starting close to each other (transient effect – concentration dependent and/or time dependent), the excited anthracene will transfer the excess charge via electron transfer to the CBr_4 molecule, quenching the excited anthracene's fluorescence.

Further fluorescence spectroscopy could be employed as further experimentation to determine whether a stable photoproduct is formed as a result of the fluorescence quenching. An excess amount of CBr_4 quencher could be mixed with anthracene in the same hexane solvent, and allowed to react in light so that all possible fluorescence quenching can occur over a relatively long period of time. This solution's fluorescence intensity at a given wavelength could then be compared to the same reaction, but with its fluorescence intensity at that specific wavelength taken immediately. If a stable (non-fluorescing) photoproduct was produced, the concentration of the anthracene would be reduced and thus produce a lower intensity measurement than the one taken immediately.

The non-polar n-hexane was used as a solvent medium because its size, as discussed in the introduction, would allow the anthracene and CBr_4 molecules to diffuse through it. If however, a polar solvent such as acetonitrile were to be used, it would directly affect the ground and excited state interactions between anthracene and CBr_4 . Specifically, the fluorescence quenching reaction occurs via the interaction between these two molecules and the transfer of electron from the

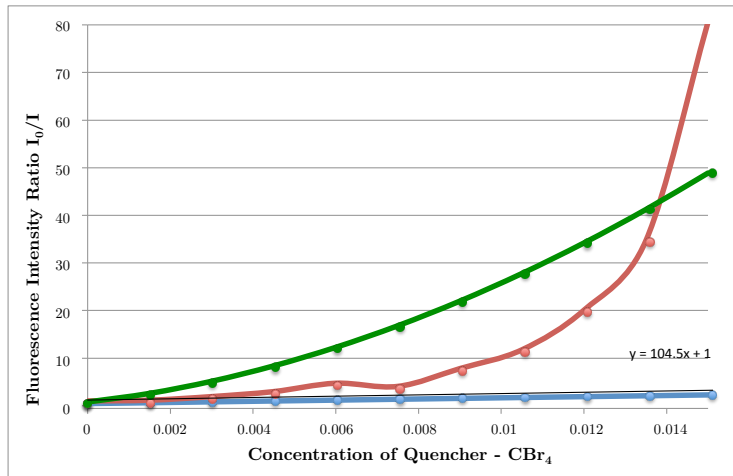
excited state anthracene to the CBr_4 quencher. A polar solvent, with uneven partial charge distributions would produce Coulombic effects, competing with the CBr_4 for the charge transfer, and thus directly affecting the rate of reaction (diffusion controlled). In addition, the ground-state anthracene and the CBr_4 diffusion through the medium towards each other to react would be affected by the uneven charge distribution of the polar solvent molecules, again affecting the rate constant.

For future experimentation, in order to maximize the transient effect, we would use a solvent of very high viscosity so that the reacting molecules that state close to each other are essentially the only ones that react (the transient effect), as the molecules that are farther away cannot successfully diffuse through the medium and thus cannot reach their collision radius and react, therefore we observe only the transient effect via only the initially nearby molecules reacting. We would also want to use an excited molecule that fluoresces with a long lifetime to confirm this. The lifetime being the fluorescing time of the excited molecule in the absence of a quencher, we would see that this high fluorescence is still observed after all the initially nearby reactants are quenched. As the high viscosity causes the excited state fluorophores to be stuck, they also have the time to fluoresce and be observed.

REFERENCES

- Atkins, P. and De Paula. *Physical Chemistry: Thermodynamics, Structure, and Change*, 10th ed. W. H. Freeman, Oxford University Press, 2014.
 - Bobok, D. and Ondrejkova, M. (1990) "Diffusion Coefficients of n-Hexane in Particles of Molecular Sieve NaY Determined by Means of Chromatographic Measurements". *Chem. Papers.* 1992 46(6) pp. 363-367.
 - Douglas, Bodie E.; Ho, Shih-Ming (2007). *Structure and Chemistry of Crystalline Solids*. New York: Springer Science+Business Media, Inc. p. 289.
 - Farley, C. D. (2017) "The Kinetics of a Diffusion Controlled Reaction – Modified Procedure".
 - Lakowicz, J. R. *Principles of Fluorescence Spectroscopy*, 3rd ed. Springer: New York, 2006.
 - Periasamy, N., Doraiswamy, S., Verkataraman, B., and Fleming, G. R. (1988) "Diffusion Controlled Reactions: Experimental Verification of the Timedependent Rate Equation". *Journal of Chemical Physics* 89, 4799 (1988); doi: 10.1063/1.455673
 - Redner, S. (1989) "Kinetics of Diffusion Controlled Reactions". *U.S. Army Research Office – Public Declassification*. DAAL03-86-K-0025
 - www.ccdc.cam.ac.uk/structures/search?id=doi:10.5517/cc7fdgh&sid=DataCite Accessed 08 May 2017
-

I_0 at 398 nm	I at 398 nm	I_0/I (Experimental)	(I_0/I) (Linearized - eq.14)	CBr_4 [Q] (M)	I_0/I (Theoretical - eq. 15)	Square Difference for I_0/I	a	b	Y
33.41	33.41	1	1.00E+00	0	1.00E+00	0	1.81E+08	0.00E+00	1.00E+00
27.23	23.54	1.15675446	1.18E+00	0.0015	2.81E+00	2.745695254	3.14E+08	5.19E+03	6.16E-01
34.4	17.97	1.914301614	1.36E+00	0.003	5.36E+00	11.88777676	4.47E+08	1.04E+04	4.60E-01
39.66	13.38	2.964125561	1.55E+00	0.0045	8.60E+00	31.71981203	5.80E+08	1.56E+04	3.72E-01
40.86	8.659	4.718789699	1.73E+00	0.006	1.25E+01	60.39517004	7.12E+08	2.08E+04	3.15E-01
35.71	8.802	4.057032493	1.91E+00	0.0075	1.70E+01	168.2676119	8.45E+08	2.60E+04	2.74E-01
35.57	4.561	7.798728349	2.09E+00	0.009	2.22E+01	207.4443368	9.78E+08	3.12E+04	2.43E-01
36.23	3.085	11.7439222	2.28E+00	0.0105	2.80E+01	264.3051002	1.11E+09	3.63E+04	2.19E-01
37.04	1.845	20.07588076	2.46E+00	0.012	3.44E+01	205.8290883	1.24E+09	4.15E+04	1.99E-01
35.57	1.024	34.73632813	2.64E+00	0.0135	4.15E+01	45.22478434	1.38E+09	4.67E+04	1.83E-01
35.57	0.441	80.65759637	2.82E+00	0.015	4.91E+01	994.9928673	1.51E+09	5.19E+04	1.70E-01



Reference Parameter	Value	Units
D (diffusion coeff. Hexane) 20C	3.06E-05	$\text{cm}^2 \text{s}^{-1}$
Avogadro's Number N_A	6.02E+23	N/A
Lifetime τ_0	5.52E-09	seconds

Equation 15 Variables	Value	Units
$4\pi D$	3.84E-04	
$N_A/1000$	6.02E+20	N/A
π	3.141592654	N/A

Targets and Variation Parameter	Value	Units
R (collision radius)	3.83E-07	cm
Sum of Square Difference	1.99E+03	

Procedure Step	Equation Used	Calculated Parameter	Numerical Value	Units
3 SES - eq. 11	k_1		2.20E+10	$\text{dm}^3 \text{ mol}^{-1} \text{ s}^{-1}$
3	D (diffusion coeff. Hexane) 20C		3.06E-05	$\text{cm}^2 \text{ s}^{-1}$
3 eq. 10	R (collision radius)	9.53E-08	cm	9.53 Å
4 eq. 14	K_{SV} (Stern-Volmer Constant)	1.22E+02	$\text{dm}^3 \text{ mol}^{-1}$	
5 eq. 14	k_1	1.89E+10	$\text{dm}^3 \text{ mol}^{-1} \text{ s}^{-1}$	
5 eq. 10	R (collision radius)	8.19E-08	cm	8.19 Å

Reference Parameter	Value	Units
R (universal gas constant)	8.31E+07	$\text{erg mol}^{-1} \text{ K}^{-1}$
Viscosity of n-hexane 25C	0.003	Poise
Room Temp.	298	K
D (diff. coeff. Heptane) 25C	4.35E-05	$\text{cm}^2 \text{ s}^{-1}$
Viscosity of n-heptane 20C	0.0042	Poise
Diffusion Constant (step 3)	3.034642857	
Avogadro's Number N_A	6.02E+23	N/A
Lifetime τ_0	5.52E-09	seconds